

## Multirate delivery of multiple therapeutic agents from metal-organic frameworks

Alistair C. McKinlay, Phoebe K. Allan, Catherine L. Renouf, Morven J. Duncan, Paul S. Wheatley, Stewart J. Warrender, Daniel Dawson, Sharon E. Ashbrook, Barbara Gil, Bartosz Marszalek, Tina Düren, Jennifer J. Williams, Cedric Charrier, Derry K. Mercer, Simon J. Teat, and Russell E. Morris

Citation: *APL Materials* **2**, 124108 (2014); doi: 10.1063/1.4903290

View online: <http://dx.doi.org/10.1063/1.4903290>

View Table of Contents: <http://scitation.aip.org/content/aip/journal/aplmater/2/12?ver=pdfcov>

Published by the [AIP Publishing](#)

---

### Articles you may be interested in

[Sonosensitive nanoparticles for controlled instigation of cavitation and drug delivery by ultrasound](#)

*AIP Conf. Proc.* **1481**, 426 (2012); 10.1063/1.4757372

[Modeling of hyaluronic acid containing anti-cancer drugs-loaded polylactic-co-glycolic acid bioconjugates for targeted delivery to cancer cells](#)

*AIP Conf. Proc.* **1482**, 75 (2012); 10.1063/1.4757441

[MAPLE deposited polymeric blends coatings for controlled drug delivery](#)

*AIP Conf. Proc.* **1464**, 547 (2012); 10.1063/1.4739908

[Preparation and characterization of conjugated polyamidoamine-MPEG-methotrexate for potential drug delivery system](#)

*AIP Conf. Proc.* **1455**, 70 (2012); 10.1063/1.4732473

[Thin films of polymer blends for controlled drug delivery deposited by matrix-assisted pulsed laser evaporation](#)

*Appl. Phys. Lett.* **96**, 243702 (2010); 10.1063/1.3453756

---



## Multirate delivery of multiple therapeutic agents from metal-organic frameworks

Alistair C. McKinlay,<sup>1</sup> Phoebe K. Allan,<sup>1</sup> Catherine L. Renouf,<sup>1</sup>  
Morven J. Duncan,<sup>1</sup> Paul S. Wheatley,<sup>1</sup> Stewart J. Warrender,<sup>1</sup>  
Daniel Dawson,<sup>1</sup> Sharon E. Ashbrook,<sup>1</sup> Barbara Gil,<sup>2</sup> Bartosz Marszalek,<sup>2</sup>  
Tina Düren,<sup>3</sup> Jennifer J. Williams,<sup>3</sup> Cedric Charrier,<sup>4</sup> Derry K. Mercer,<sup>4</sup>  
Simon J. Teat,<sup>5</sup> and Russell E. Morris<sup>1</sup>

<sup>1</sup>*EaStCHEM School of Chemistry, University of St Andrews,  
St Andrews KY16 9ST, United Kingdom*

<sup>2</sup>*Faculty of Chemistry, Jagiellonian University, Ingardena 3, 30-060 Kraków, Poland*

<sup>3</sup>*School of Engineering, Institute for Materials and Processes, The University of Edinburgh,  
Edinburgh EH9 3JL, United Kingdom*

<sup>4</sup>*NovaBiotics Ltd., Cruickshank Building, Craibstone, Aberdeen AB21 9TR, United Kingdom*

<sup>5</sup>*Advanced Light Source, Lawrence Berkeley National Laboratory, 1 Cyclotron Road,  
Mail Stop 15-317, Berkeley, California 94720, USA*

(Received 20 June 2014; accepted 20 November 2014; published online 11 December 2014)

The highly porous nature of metal-organic frameworks (MOFs) offers great potential for the delivery of therapeutic agents. Here, we show that highly porous metal-organic frameworks can be used to deliver multiple therapeutic agents—a biologically active gas, an antibiotic drug molecule, and an active metal ion—simultaneously but at different rates. The possibilities offered by delivery of multiple agents with different mechanisms of action and, in particular, variable timescales may allow new therapy approaches. Here, we show that the loaded MOFs are highly active against various strains of bacteria. © 2014 Author(s). All article content, except where otherwise noted, is licensed under a Creative Commons Attribution 3.0 Unported License. [<http://dx.doi.org/10.1063/1.4903290>]

Metal-organic frameworks (MOFs) are some of the most exciting chemical entities to have emerged in science over the last decade or so.<sup>1</sup> They are solids comprised of metal or metal-cluster nodes linked by organic ligands into three-dimensional networks, which often have very high porosity in the nanopore (micropore to mesopore) regime. These materials have aroused much excitement for their ability to adsorb very large quantities of fuel vector gases such as hydrogen and methane,<sup>2,3</sup> environmental gases such as carbon dioxide,<sup>4</sup> as well as for their fundamental properties in other areas.<sup>5–7</sup> In recent times, their very high adsorption capacities coupled with their chemical flexibility, which allow the preparation of toxicologically acceptable variants, has led to a burgeoning interest in using MOFs to adsorb and deliver large payloads of therapeutic agents,<sup>8–10</sup> notably anti-cancer drug molecules and biologically active gases<sup>11,12</sup> and there is even an example of anti-cancer drugs and gases being delivered simultaneously.<sup>13</sup>

The administration of more than one therapeutic agent to treat a single disease, often called combination therapy, is an increasing feature of medicine.<sup>14</sup> Such a treatment strategy is used when the various therapeutic agents work together in some manner or when features such as drug resistance need to be prevented or overcome. In this paper, we show how the extremely large capacity for guests inherent in MOFs can be combined with their chemical composition to give materials that deliver multiple therapeutic agents. The interest in this type of system comes from the different rates at which the various agents are released and the different mechanisms of action of the various agents. We show that in antibacterial studies, the method is effective even when one component of the material is less active against particular strains of bacteria, offering a way to avoid the issues associated with resistance.



The great advantage of MOFs as delivery agents lies in their structural architecture and in their chemical (and structural) diversity. The concept of BioMOFs, materials with properties that can be used for biological and medical applications, is beginning to gain traction in the community. An explosion in MOF synthesis over the last few years means there are hundreds of potentially interesting structures in this family. In our preliminary work, we have concentrated on two materials—the so-called M-CPO-27 (MOF-74) series of materials<sup>15,16</sup> and the copper-based HKUST-1 (CuBTC) structure.<sup>17,18</sup> Both have relatively high porosity combined with the potential for the production of undercoordinated metal sites (sometimes called open metal sites). In this paper, we show that both M-CPO-27 and HKUST-1 can be used to deliver multiple therapeutic agents, before concentrating on Ni-CPO-27 as a material with particularly good properties.

The M-CPO-27 family of materials (Figure 1) is formed from linking metals (M = Mg, Fe, Mn, Co, Ni, or Zn) with a 2,5-dihydroxyterephthalate linker. The 11 Å diameter one-dimensional channels coupled with highly accessible under-coordinated metal ions lead to some excellent properties for gas adsorption and separation.<sup>9,19,20</sup> The biological properties of the metals range from very toxic (Co) to relatively benign (Fe and Mg). Metal ions such as Ni<sup>2+</sup> and Zn<sup>2+</sup>, however, have established antimicrobial behaviour, and so these MOFs have the potential to be antibacterial. HKUST-1 is a copper benzene-1,3,5-tricarboxylate with a three-dimensional pore system. The copper ions in the solid are highly accessible and can be undercoordinated on activation (desolvation).

The anti-bacterial properties of MOFs themselves are very little studied,<sup>21</sup> but as they are generally known to be slightly unstable in aqueous solutions (although this varies from one MOF structure to the next), we would expect the MOFs to deliver metal ions into the environment and so act as antibacterial agents in their own right. However, the high porosity in MOF structures can also be used to store and deliver biologically active guests. The Ferey and Lin groups<sup>22–24</sup> have recently shown how MOFs can be utilised to adsorb and deliver extremely large quantities of anti-cancer and other drugs, or be used in diagnosis. Similarly, M-CPO-27 MOFs also show exceptional performance for the delivery of therapeutic gases such as nitric oxide (NO) and hydrogen sulfide (H<sub>2</sub>S).<sup>25,26</sup> HKUST-1 is less good at delivering NO, but does deliver enough for certain applications (e.g., prevention of platelet activation).<sup>18</sup> Going beyond even this, in this paper, we show that M-CPO-27 and HKUST-1 MOFs that are active in their own right can be used to store and release multiple agents, such as a biologically active gas (NO) and an antibiotic molecule, simultaneously.

We show how the multirate delivery from the materials allows a strategy for anti-bacterial action that delivers a burst of a powerful, fast-acting bactericidal agent, such as NO, to kill the majority of bacteria while allowing the microbial burden on the materials to be kept low through the slower, staged delivery of other agents. Larger anti-bacterial guest molecules such as the antibiotic metronidazole are delivered more slowly than NO, and finally the metal ions are delivered even more slowly still. The materials are extremely active against both Gram positive and Gram negative bacteria.

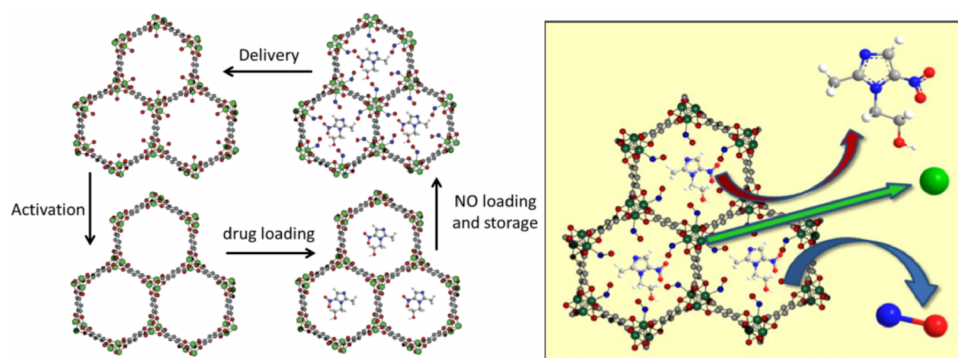


FIG. 1. The assembly strategy for loading of multiple therapeutic agents in MOFs. The loading of the guests is a stepwise process; activation (the thermal dehydration) followed by loading of a drug (in this case, the antibiotic metronidazole). A further activation step (not explicitly shown) is then followed by loading of the gas (in this case, nitric oxide). Delivery of the therapeutic agents is then triggered by exposure to water.

The MOFs M-CPO-27 ( $M = \text{Ni}, \text{Co}$ ) and HKUST-1 were prepared as described in the literature.<sup>13,15,27</sup> The as-prepared MOFs were then loaded with the required guest species, using either solution (e.g., for antibiotic drug molecules) or gas phase (e.g., for NO) methods as described in the methods section and in the supplementary information.<sup>28</sup> Special care has to be taken when loading both antibiotic molecules and NO (Figure 1). In this case, the antibiotics are loaded into a previously desolvated (activated) MOF using the appropriate solution state method followed by a second activation step that removes any solvent that has been co-occluded into the MOF. In general, the first activation step is carried out at 120 °C and the second at a lower temperature (80 °C) to prevent thermal desorption of the antibiotic drug molecule (Figure 1).

A calculated amount of Ni CPO-27 or HKUST-1 was activated and stored using the procedure described earlier. 100 mg of metronidazole was added into a sample vial and 10 ml of dry methanol was added. Once the drug had fully dissolved in the solvent, the dehydrated MOF sample was added to the sample vial and the mixture was left stirring for 3 days. Using a variety of characterisation methods (thermogravimetric analysis (TGA), IR, and solid state NMR), it was shown that the drugs had indeed been adsorbed inside the pores of the material. A combination of elemental analysis and TGA indicates that the materials adsorb between 0.11 and 0.16 g metronidazole per gram of dry MOF.

Loading of NO powdered samples of the MOFs (~0.03 g) was reactivated under vacuum at 80 °C to remove any solvent that had been co-adsorbed as described above. The MOFs were then cooled to room temperature and exposed to approximately 2 atm of dry NO (99.5%, Air Liquid) for 30 min, evacuated and exposed to dry argon. Evacuation and exposure to NO was repeated three times.

NO release measurements were performed using a Sievers NOA 280i chemiluminescence Nitric Oxide Analyser. The instrument was calibrated by passing air through a zero filter (Sievers, <1 ppb NO) and 89.48 ppm NO gas (Air Products, balance nitrogen). The flow rate was set to 180 ml/min with a cell pressure of 8.5 Torr and an oxygen pressure of 6.1 psig. For experiments in

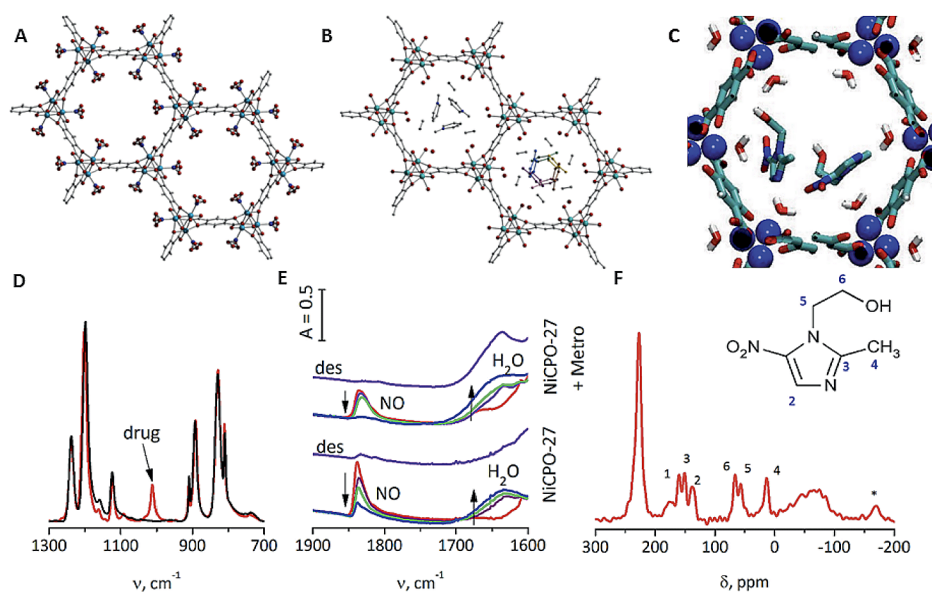


FIG. 2. Characterisation of multiple-guest loaded MOFs. (a) shows the single crystal structure of NO-loaded CPO-27. (b) is the partial crystal structure of metronidazole-loaded CPO-27, identifying the location of the five-membered ring in the centre of the channels. (c) is a computer simulation of metronidazole inside the pores of the CPO-27 framework, indicating that there is enough space to accommodate the drug even when there is a molecule attached to the metal ions (in this case, water mimicking the solid after release of NO). (d) shows the IR spectrum of the NO/metronidazole-loaded CPO-27 (red) compared to the empty Ni-CPO-27 (black). (e) is the IR spectrum of Ni-CPO-27 (bottom) and Metronidazole loaded Ni-CPO-27 after exposure to NO, and on subsequent exposure to water. (f) is the <sup>13</sup>C MAS NMR spectrum of NO/metronidazole-loaded HKUST-1 showing clearly the resonances due to the drug molecule.

contact with phosphate buffered saline, calculated amounts of each MOF were ground together with Teflon (10 wt. %) and this mixture was then pressed into 5 mm pellets, which were then dehydrated and loaded with NO in the same way as the powder samples. The pellets were placed in a sample vial which was capped and then PBS buffer solution was then injected (4 ml). The NO released was measured in the same manner as above.

The same sample used in the NO release measurements was also used to follow the release of the metronidazole drug molecules and the metal ions from the MOF. At regular time points, a small aliquot of the PBS sample was taken from the main sample and UV spectroscopy used to measure the concentration of metronidazole present. The metal concentrations in the liquids were also measured using atomic adsorption.

Both HKUST-1 and the M-CPO-27 (M = Ni and Co) family of materials are good at binding large quantities of NO, and then releasing it on exposure to a moisture trigger in biologically active quantities.<sup>12,18</sup> M-CPO-27 is particularly attractive for gas delivery applications of this kind as it has a large number of coordinatively unsaturated metal sites lining the pore walls in the MOFs, to which the NO bonds strongly<sup>12</sup> and we have therefore concentrated our characterisation on this material. This is clearly seen in the single crystal X-ray diffraction experiment on NO-loaded Co-CPO-27 (Figure 2(a)), and is confirmed by infrared adsorption spectroscopy on the Ni-CPO-27 (Single crystal X-ray diffraction studies cannot be completed on the Ni-CPO-27 because the crystals are not large enough). An added feature of the M-CPO-27 structure is its high pore volume, and large channels that can be used to adsorb small and medium-sized drug molecules. The antibiotic molecule, metronidazole, which is used to treat *Clostridium difficile* and various parasitic infections, can be adsorbed into the pores of M-CPO-27 in large amounts (See supplementary material). Single crystal X-ray diffraction experiments on the metronidazole-loaded Co-CPO-27 revealed a partial structure of the molecule in the channels, allowing location of the five-membered ring of the drug but not the heavily disordered side chains (Figure 2(b)). The crystallographic information file for this structure determination can be found as supplementary information. However, it is striking when comparing the two single crystal structures (Figs 2(a) and 2(b)) that the NO and the drug do not occupy the same space in the material, opening up the possibility of having both NO and metronidazole as guests in the M-CPO-27 simultaneously. We also completed some simple computer simulations to show that the location of the metronidazole found in the partial crystal structure is consistent with the modelling studies and to show that there is a space for both metronidazole and species attached to the open metal sites (such as water, as shown in Figure 2(c), and methanol—the solvent used to load the drug). Water is particularly important as exposure to moisture is the mechanism by which NO is released from MOFs.<sup>12</sup>

In order to probe whether both NO and metronidazole could be accommodated by the structure at the same time, a specified number of NO and metronidazole molecules was inserted at random positions within the MOF using Gromacs. Ni-CPO-27 was loaded with 45 metronidazole molecules per simulation cell (corresponding to a loading of 0.5 mmol/g) and 200 molecules of NO per simulation cell. The criterion for successful insertion of a molecule was that the distance between any atom of the inserted molecule and any atom already present in the MOF framework was less than the sum of the van der Waals radii of both atoms. The larger metronidazole molecule/s were inserted first followed by the NO molecules. This simulation work indicated that there was sufficient space inside the pores for both species to be accommodated in close proximity to each other (i.e., in the same unit cell). Similar simulations also showed that water and methanol could also be accommodated in the same pore space as the metronidazole.

To load multiple guest samples of Ni-CPO-27 and HKUST-1, they were first activated thermally and then exposed to a solution of metronidazole in dry methanol and the subsequent metronidazole-loaded MOFs were then subjected to a further activation step at 80 °C under vacuum, before being exposed to ~2 atm of NO gas. That the resultant MOFs were successfully loaded with both metronidazole and NO was proved through infrared and magic-angle spinning (MAS) NMR (nuclear magnetic resonance) experiments and through measurement of the delivery of the different agents.

Infrared and MAS NMR spectroscopies were used to characterise the multiply loaded MOFs. Both the NO and the drugs can be clearly identified in the IR spectra (Figures 2(d) and 2(e)) of the

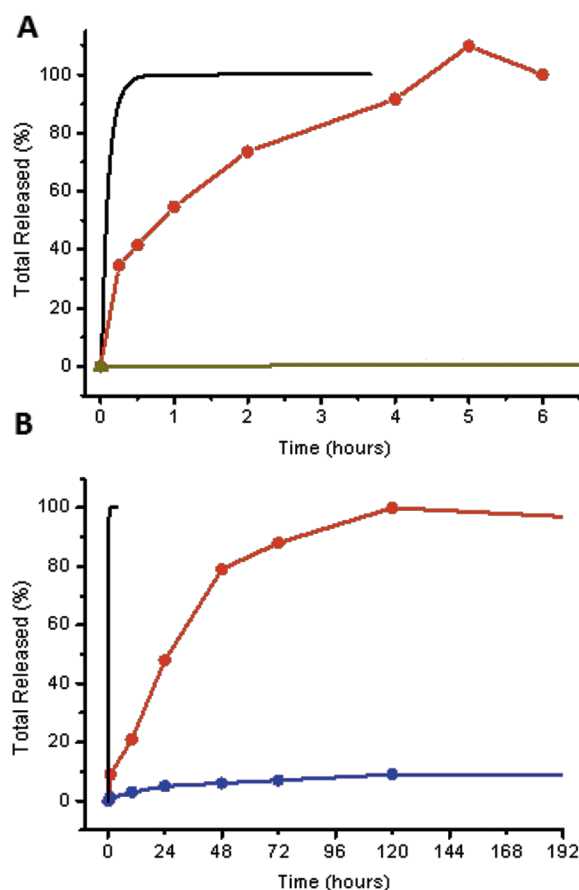


FIG. 3. Relative rates of release of NO, metronidazole, and metal ions. Delivery from (a) Ni-CPO-27 and (b) HKUST-1 (note the difference in scales between the samples). Key: black line = NO release, red line = metronidazole release, green line = Ni release, and blue line = Cu release. <4% of the Ni is lost after 6 h. Note that the error on the drug measurement is about  $\pm 5\%$ . Errors on the NO and the metal release are much smaller ( $\sim 1\%$ ). Note that the  $t = 5$  h point in Figure (a) shows an unfeasibly high value for metronidazole release and should be treated as an outlier.

CPO-27 structures, while the resonances due to the drug molecule itself are easily identified in  $^{13}\text{C}$  MAS NMR experiments on HKUST-1 (Figure 2(f), note that the NMR spectrum of Ni-CPO-27 and NO-loaded materials are very difficult to obtain because of the highly paramagnetic nature of the materials). The presence of metronidazole in the pores affects the delivery of the NO on contact with moisture (Figure 3). Without metronidazole, the NO is quickly accessible to even the smallest amount of water (see Refs. 12 and 18 for these studies). However, the amount of water required to show a diminution of the NO band is larger when metronidazole is present. Nevertheless, all the NO is released.

The relative rates of release of the three therapeutic agents from the MOFs were measured in both water and phosphate buffered saline (PBS) in order to mimic the release of the agents in different situations. The NO release was measured using chemiluminescence methods, the release of the metronidazole was quantified using ultraviolet spectroscopy, and the release of the metal ions into solution was measured using atomic absorption spectroscopy. The relative rates of delivery in contact with water and PBS are broadly similar. Larger changes in the relative rates of delivery are seen by altering the structure of the MOF. For example, Figure 3 shows the relative rates of delivery of NO, metronidazole, and metal ions from Ni-CPO-27 and HKUST-1. For Ni-CPO-27, the NO ( $\sim 2 \text{ mmol g}^{-1}$ ) is delivered quickly, completed after  $\sim 30$  min, the metronidazole ( $0.2 \text{ mmol g}^{-1}$ ) more slowly (completed after  $\sim 6$  h), and the metal ions ( $\sim 0.09 \text{ mmol g}^{-1}$ ) much more slowly still (after 6 h only 4% of the possible metal ions have been released). Note that the maximum amount of

NO adsorbed in the pre-drug loaded MOFs is naturally lower than the amount that can be adsorbed into “empty” MOFs.<sup>12,18</sup>

The delivery of NO from HKUST-1 is complete after around 2 h. The metronidazole is slowed down even more, with completion delayed until around ~120 h. The delivery of the metal ions is, however, comparable in rate to that of M-CPO-27. This shows that there is scope not only to deliver multiple agents at different rates from MOFs but also to tailor the relative delivery rates (particularly of the drug) by using different MOF structure types. Molecular dynamics studies (see supplementary information for further information) of the materials containing both NO and metronidazole in the Ni-CPO-27 structure confirm that the simulated rate of self-diffusion of NO in Ni-CPO-27 ( $21\,047 \times 10^{-8} \text{ cm s}^{-1}$ ) is considerably greater than the self-diffusion of metronidazole ( $2.7 \times 10^{-8} \text{ cm s}^{-1}$ ).

As well as the relative rates of delivery of the various agents, the absolute amount of NO or drug delivered can also be tailored by choice of the framework itself. HKUST-1 delivers significantly less NO,<sup>12,18</sup> but those similar amounts of metronidazole can be stored in and delivered from HKUST-1 (~0.3–0.5 mmol g<sup>-1</sup> compared to between 0.5 and 0.9 mmol g<sup>-1</sup> for Ni-CPO-27).

As described above, metronidazole is the antibiotic of choice for treatment of *C. difficile* and parasitic infections. However, it is known to be less active against other organisms when dosed in therapeutically relevant amounts. This offers an excellent test of the multi-agent combination approaches we describe here, as a way of mitigating against resistance to any one agent. In this way, we have tested the NO/metronidazole-loaded MOFs against *Pseudomonas aeruginosa* (strains PAO1 and Pa058) and *Staphylococcus aureus* (DSMZ11729). *P. aeruginosa* and *S. aureus* represent two of the six ESKAPE (shorthand for the family of bacteria containing *Enterococcus faecium*, *Staphylococcus aureus*, *Klebsiella pneumoniae*, *Acinetobacter baumannii*, *Pseudomonas aeruginosa*, and *Enterobacter* species) pathogens recently highlighted as the cause of the majority of US hospital-acquired infections and for which antibiotic resistance is becoming an increasing problem.<sup>29</sup> For the antibacterial tests, the MOFs were prepared as small disks in a blend with polytetrafluoroethylene (PTFE) (total mass ~20 mg), allowing the amount of MOF (and so the dose of antibacterial agent) to be varied while keeping the size of the test item constant (further details can be found in the supplementary material). A PTFE disk of the same size containing no MOF was used as a control. The reduction in metabolic activity was monitored, assessment taking place over 20 h.

Antimicrobial susceptibility testing to determine the growth inhibition by the test items was carried out using modifications of the Clinical and Laboratory Standards Institute (CLSI) broth microdilution procedure.<sup>30</sup> The MOFs were not optically transparent and therefore did not permit kinetic analysis of microbial growth by changes in optical density. Therefore, the above CLSI protocol was adapted to monitor microbial metabolic activity using Alamar blue (a cell viability indicator), which detected changes in metabolic activity, rather than optical density.

Figure 4 shows representative results of the antibacterial testing carried out over 20 h against *P. aeruginosa* PAO1 and *S. aureus* DSMZ11729. MOFs with antibacterial metals Ni in M-CPO-27 and Cu in HKUST-1 showed significant antibacterial activity against all the strains of bacteria tested when in large amounts (e.g., 16 mg of MOF). As the amount of MOF is reduced, however, down to levels of 1–2 mg of MOF, the efficacy is reduced. Taking the results of Ni-CPO-27 against *S. aureus* as an example (Figure 4(b)), the MOF itself is partially effective when compared to the control (vancomycin). The same experiment with a MOF loaded with metronidazole shows no improvement in antibacterial activity, as would be expected. In fact, the activity is slightly worse, probably caused by the organic molecule in the channels hindering the release of metal ions into the solution. Repeating the same experiments with both metronidazole and NO in the MOF showed a significant increase in antibacterial activity, with bacterial levels significantly below the levels attained when dosed with vancomycin. At all stages during the experiment, no metabolic activity was detected, indicating that the NO/metronidazole loaded MOF is rapidly bactericidal at all times. Similar results were seen against all strains of bacteria tested. The synergy of the different rates of release is most evident when the materials are re-challenged with bacteria successively. Even after all NO has been released, the materials remain active, demonstrating that metal ion release is still occurring and still reducing the bacterial burden up to 10 days after the experiment is started.

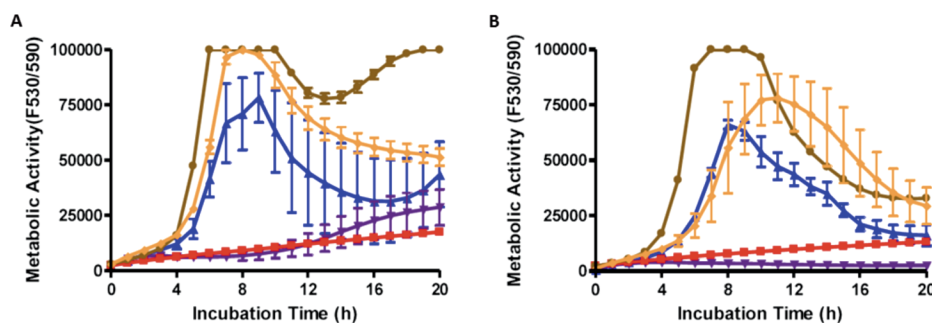


FIG. 4. The anti-bacterial activity of Ni-CPO-27 against planktonic *P. aeruginosa* and *S. aureus*, respectively. Key for (a) and (b): brown line = growth control; blue = MOF only, orange = metronidazole-loaded MOF; purple = NO- and metronidazole-loaded MOF; and red line = antibiotic control.

Here, we have shown how the large porosity in metal organic frameworks leads to the possibility for the design of multifunctional antimicrobial agents through the delivery of anti-bacterial gases, antibiotic molecules, and anti-bacterial metal ions. The rates of delivery from the MOFs are different, enabling a strategy that allows for both fast and long-lived bactericidal action.

However, it should be noted that this strategy is not limited to anti-bacterial agents, or even to agents that have the same intended activity. For instance, the combination therapy approach could easily include any drug molecule in combination with metal-ions and/or biologically active gases, which can themselves, have different activities. A wide range of different drug molecules can be adsorbed into and delivered from MOFs with actions ranging from anti-cancer to anti-inflammatory and analgesic.<sup>22–24</sup> MOFs loaded with any of these drugs can also be loaded with NO leading to trifunctional materials. For example, caffeine and ibuprofen can be loaded into both HKUST-1 and Ni-CPO-27 in high amounts followed by adsorption of NO. This leads to MOFs with antibacterial as well as other activity. In fact, a particular example of potentially important synergy is the combination of NO, which is not only antibacterial but is also a strong vasodilator, i.e., it increases blood flow via relaxation of blood vessels.<sup>31</sup> For topical applications, which is our main target in the work we report here, the combination of a drug (e.g., caffeine) with NO could lead to material that has three different activities—antibacterial, vasodilator, and caffeine-specific metabolic stimulation—with the vasodilatory action of the NO potentially improving the adsorption of the drug through the skin simply by increasing blood flow. Of course, questions still remain regarding the toxicity of MOF materials (especially with regard to the nickel ions). However, preliminary cytotoxicity experiments (see the supplementary material) suggest that in experiments on dermal fibroblasts, the concentration of MOF that is toxic is considerably greater than the minimum amount needed to be antibacterial.<sup>32</sup> This means that there is a potential window in which these materials might be toxicologically acceptable. However, even with suitable acute toxicity, it may be that the long-term toxicity of the metal (and indeed the linkers) in MOFs needs to be further studied before we can truly develop new medical applications of these materials.

The strategy reported here relies on the large pore volumes available in MOFs, which are not generally available in any other class of materials, enabling new strategies for drug delivery to be developed.

R.E.M. is a Royal Society Industry Fellow and thanks the Royal Society for the provision of the Brian Mercer Award for Innovation, and thanks Scottish Enterprise for support. R.E.M. also thanks the British Heart Foundation for a New Horizons Award (NH/11/8/29253). R.E.M. and T.D. thank the EPSRC for funding (EP/K025112/1 and EP/K005499/1). The IR studies (B.G. and B.M.) were carried out with the equipment purchased thanks to the financial support of the European Regional Development Fund in the framework of the Polish Innovation Economy Operational Program (Contract No. POIG.02.01.00-12-023/08). The Advanced Light Source is supported by the Director, Office of Science, Office of Basic Energy Sciences, of the U.S. Department of Energy under Contract No. DE-AC02-05CH11231.



- <sup>1</sup> J. R. Long and O. M. Yaghi, *Chem. Soc. Rev.* **38**, 1213 (2009).
- <sup>2</sup> N. L. Rosi, J. Eckert, M. Eddaoudi, D. T. Vodak, J. Kim, M. O'keeffe, and O. M. Yaghi, *Science* **300**, 1127 (2003).
- <sup>3</sup> M. Eddaoudi, J. Kim, N. Rosi, D. Vodak, J. Wachter, M. O'keeffe, and O. M. Yaghi, *Science* **295**, 469 (2002).
- <sup>4</sup> B. Wang, A. P. Cote, H. Furukawa, M. O'keeffe, and O. M. Yaghi, *Nature* **453**, 207 (2008).
- <sup>5</sup> C. Serre, C. Mellot-Drazniéks, S. Surble, N. Audebrand, Y. Filinchuk, and G. Férey, *Science* **315**, 1828 (2007).
- <sup>6</sup> B. Xiao, P. J. Byrne, P. S. Wheatley, D. S. Wragg, X. Zhao, A. J. Fletcher, K. M. Thomas, L. Peters, J. S. O. Evans, J. E. Warren, W. Zhou, and R. E. Morris, *Nat. Chem.* **1**, 289 (2009).
- <sup>7</sup> M. I. H. Mohideen, B. Xiao, P. S. Wheatley, A. C. McKinlay, Y. Li, A. M. Z. Slawin, D. W. Aldous, N. F. Cessford, T. Dueren, X. Zhao, R. Gill, K. M. Thomas, J. M. Griffin, S. E. Ashbrook, and R. E. Morris, *Nat. Chem.* **3**, 304 (2011).
- <sup>8</sup> P. Horcajada, R. Gref, T. Baati, P. K. Allan, G. Maurin, P. Couvreur, G. Férey, R. E. Morris, and C. Serre, *Chem. Rev.* **112**, 1232 (2012).
- <sup>9</sup> A. C. McKinlay, R. E. Morris, P. Horcajada, G. Férey, R. Gref, P. Couvreur, and C. Serre, *Angew. Chem.* **49**, 6260 (2010).
- <sup>10</sup> J. D. Rocca, D. Liu, and W. Lin, *Acc. Chem. Res.* **44**, 957 (2011).
- <sup>11</sup> P. Horcajada, T. Chalati, C. Serre, B. Gillet, C. Sebrie, T. Baati, J. F. Eubank, D. Heurtaux, P. Clayette, C. Kreuz, J.-S. Chang, Y. K. Hwang, V. Marsaud, P.-N. Bories, L. Cynober, S. Gil, G. Férey, P. Couvreur, and R. Gref, *Nat. Mater.* **9**, 172 (2010).
- <sup>12</sup> A. C. McKinlay, B. Xiao, D. S. Wragg, P. S. Wheatley, I. L. Megson, and R. E. Morris, *J. Am. Chem. Soc.* **130**, 10440 (2008).
- <sup>13</sup> S. Rojas, P. S. Wheatley, E. Quartapelle-Procopio, B. Gil, B. Marszalek, R. E. Morris, and E. Barea, *CrystEngComm* **15**, 9364 (2013).
- <sup>14</sup> J. Jia, F. Zhu, X. Ma, Z. W. Cao, Y. X. Li., and Y. Z. Chen, *Nat. Rev. Drug Discovery* **8**, 111 (2009).
- <sup>15</sup> P. D. C. Dietzel, Y. Morita, R. Blom, and H. Fjellvåg, *Angew. Chem.* **44**, 6354 (2005).
- <sup>16</sup> N. L. Rosi, J. Kim, M. Eddaoudi, B. L. Chen, M. O'keeffe, and O. M. Yaghi, *J. Am. Chem. Soc.* **127**, 1504 (2005).
- <sup>17</sup> S. S. Y. Chui, S. M. F. Lo, J. P. H. Charmant, A. G. Orpen, and I. D. Williams, *Science* **283**, 1148 (1999).
- <sup>18</sup> B. Xiao, P. S. Wheatley, X. Zhao, A. J. Fletcher, S. Fox, A. G. Rossi, I. L. Megson, S. Bordiga, L. Regli, K. M. Thomas, and R. E. Morris, *J. Am. Chem. Soc.* **129**, 1203 (2007).
- <sup>19</sup> E. D. Bloch, W. L. Queen, R. Krishna, J. M. Zadrozny, C. M. Brown, and J. R. Long, *Science* **335**, 1606 (2012).
- <sup>20</sup> D. Britt, H. Furukawa, B. Wang, T. G. Glover, and O. M. Yaghi, *Proc. Natl. Acad. Sci. U. S. A.* **106**, 20637 (2009).
- <sup>21</sup> X. Y. Lu, J. W. Ye, D. K. Zhang, R. X. Xie, R. F. Bogale, Y. Su, L. M. Zhao, Q. Zhao, and G. L. Ning, *J. Inorg. Biochem.* **138**, 114 (2014).
- <sup>22</sup> P. Horcajada, C. Serre, G. Maurin, N. A. Ramsahye, F. Balas, M. Vallet-Regi, M. Sebban, F. Taulelle, and G. Férey, *J. Am. Chem. Soc.* **130**, 6774 (2008).
- <sup>23</sup> P. Horcajada, C. Serre, M. Vallet-Regi, M. Sebban, F. Taulelle, and G. Férey, *Angew. Chem.* **45**, 5974 (2006).
- <sup>24</sup> R. C. Huxford, J. D. Rocca, and W. Lin, *Curr. Opin. Chem. Biol.* **14**, 262 (2010).
- <sup>25</sup> N. J. Hinks, A. C. McKinlay, B. Xiao, P. S. Wheatley, and R. E. Morris, *Microporous Mesoporous Mater.* **129**, 330 (2010).
- <sup>26</sup> P. K. Allan, P. S. Wheatley, D. Aldous, M. I. Mohideen, C. Tang, J. A. Hriljac, I. L. Megson, K. W. Chapman, G. De Weireld, S. Vaesen, and R. E. Morris, *Dalton Trans.* **41**, 4060 (2012).
- <sup>27</sup> P. D. C. Dietzel, R. Blom, and H. Fjellvåg, *Eur. J. Inorg. Chem.* **23**, 3624 (2008).
- <sup>28</sup> See supplementary material at <http://dx.doi.org/10.1063/1.4903290> for details of the synthesis, loading, and characterization of the materials.
- <sup>29</sup> H. W. Boucher, G. H. Talbot, J. S. Bradley, J. E. Edwards, Jr., D. Gilbert, L. B. Rice, M. Scheld, B. Spellberg, and J. Bartlett, *Clin. Infect. Dis.* **48**, 1 (2009).
- <sup>30</sup> Clinical and Laboratory Standards Institute, *Methods for Dilution Antimicrobial Susceptibility Tests for Bacteria that Grow Aerobically* Approved Standard—Ninth Edition M07–A9 (Clinical and Laboratory Standards Institute, 2012).
- <sup>31</sup> M. Mowbray, X. Tan, P. S. Wheatley, R. E. Morris, and R. B. Weller, *J. Invest. Dermatol.* **128**, 352 (2008).
- <sup>32</sup> M. J. Duncan, S. J. Warrender, and R. E. Morris, Cytotoxicity of MOFs (unpublished).